

Defect model for nonstoichiometry in $\text{YBa}_2\text{Cu}_3\text{O}_{6+y}$

A. Mehta and D. M. Smyth

Materials Research Center, Lehigh University, 5 East Packer Avenue, Bethlehem, Pennsylvania 18015-3194

(Received 13 January 1994; revised manuscript received 19 December 1994)

A simple defect model is proposed for the variable oxygen content of $\text{YBa}_2\text{Cu}_3\text{O}_x$. It is based on the single assumption that $\text{YBa}_2\text{Cu}_3\text{O}_6$ is the stoichiometric composition of a highly acceptor-doped version of the prototype compound $\text{Y}_3\text{Cu}_3\text{O}_7$. The acceptor centers, Ba'_{Y} , are compensated by oxygen vacancies at the stoichiometric composition. The oxidation reaction then involves the filling of extrinsic oxygen vacancies and creation of holes in accord with the conventional treatment of a wide variety of acceptor-doped perovskite and perovskite-related oxides. A standard mass-action treatment leads to the expression $(6+y)y^2/(1-y) = 3.594 \times 10^{-4} e^{0.83 \text{ eV}/kT} P(\text{O}_2)^{1/2}$, where y is defined by $\text{YBa}_2\text{Cu}_3\text{O}_{6+y}$, and -0.83 eV is the enthalpy of oxidation per added oxygen, in agreement with calorimetric values. This expression is in excellent agreement with published thermogravimetric data over the range $300\text{--}900^\circ\text{C}$ and $10^{-5}\text{--}1$ atm $P(\text{O}_2)$. Correction for intrinsic ionization improves the fit to the experimental data at high temperatures and low oxygen activities, i.e., for low values of y . Linear Arrhenius behavior over four orders of magnitude of the mass-action constant is indicative of ideal behavior. The proposal that $\text{YBa}_2\text{Cu}_3\text{O}_6$ is a highly acceptor-doped composition is in agreement with its insensitivity to aliovalent dopants.

INTRODUCTION

There have been several attempts to develop a defect model for the variable oxygen content of $\text{YBa}_2\text{Cu}_3\text{O}_x$ (YBCO), where $6.0 < x < 7.0$.¹⁻⁹ The goal is to fit the experimentally determined oxygen content as a function of temperature and oxygen activity. The attempts have involved various definitions of the stoichiometric composition, a variety of defects such as oxygen vacancies and oxygen interstitials in different charge states, and different oxidation states for the Cu content. Because of the extremely large amount of nonstoichiometry, there has been concern that the behavior will not be ideal and that the classical mass-action approach based on dilute-solution thermodynamics will not be adequate. Most models have treated the nonstoichiometry in terms of an essentially pure compound. This paper will review a model described in part in several publications^{2-4,7} that treats $\text{YBa}_2\text{Cu}_3\text{O}_6$ as the stoichiometric composition of a highly acceptor-doped material. The acceptor centers are Ba^{2+} ions substituted for Y^{3+} in the prototype oxide $\text{Y}_3\text{Cu}_3\text{O}_7$. It will be shown that this model leads to an accurate fit to the extensive thermogravimetric data of Lindemer *et al.*, which seem to have been collected with extreme care for full equilibration.¹⁰ The fit to the model covers the experimental range $300\text{--}900^\circ\text{C}$ and $10^{-5}\text{--}1$ atm. The model is also in accordance with the observed insensitivity of the material to aliovalent dopants.¹¹ It has not proved necessary to correct this model for nonideal behavior, but inclusion of intrinsic ionization across the band gap improves the fit to the experimental data for small values of y .

STOICHIOMETRIC COMPOSITION

Any discussion of nonstoichiometry must be based on a definition of the stoichiometric composition. That

definition is obvious for simple compounds, but for a complex material like YBCO, it is not so readily apparent. In principle, the stoichiometric composition of a complex compound corresponds to a combination of stoichiometric binary constituents. Thus the stoichiometric composition of SrTiO_3 is the combination of the stoichiometric binary oxides SrO and TiO_2 , for LiNbO_3 it is the combination of Li_2O and Nb_2O_5 , etc. However, the situation is not so clear in YBCO, because Cu_2O , CuO , and Cu_2O_3 could all be considered to be stoichiometric binary constituents. The basic definition also holds true for doped compounds; e.g., the stoichiometric composition for SrTiO_3 doped with Al_2O_3 is $\text{SrO} + (1-x)\text{TiO}_2 + (x/2)\text{Al}_2\text{O}_3$, i.e., $\text{SrTi}_{1-x}\text{Al}_x\text{O}_{3-x/2}$. The charge of the acceptor centers Al'_{Ti} is compensated by oxygen vacancies, and charge neutrality is determined by $[\text{Al}'_{\text{Ti}}] = 2[V''_{\text{O}}]$. At the stoichiometric composition of semiconducting and insulating compounds, the valence band is nominally filled and the conduction band is nominally empty, and the only source of electronic charge carriers is by ionization across the band gap, so that $n = p$. For that reason, the stoichiometric composition is usually located near a minimum in the high-temperature, equilibrium electrical conductivity, measured as a function of oxygen activity, unless the electron and hole mobilities are widely different.

The equilibrium conductivity of YBCO as a function of oxygen activity is shown in Fig. 1.¹² There is a minimum in the conductivity for temperatures above 700°C , just before the compound decomposes below 10^{-4} atm. Comparison with compositional data, e.g., that of Lindemer *et al.*,¹⁰ shows that the minima occur very close to the composition $\text{YBa}_2\text{Cu}_3\text{O}_6$. Therefore this will be taken as the stoichiometric composition, in agreement with the opinion of most other authors,^{1,9} and the system will be treated as $\text{YBa}_2\text{Cu}_3\text{O}_{6+y}$, with $0 < y < 1$.

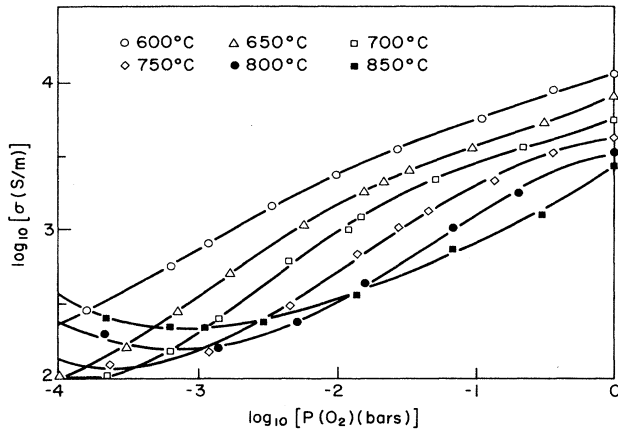


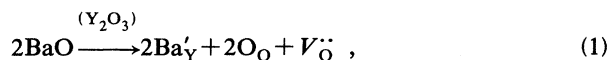
FIG. 1. Equilibrium conductivity of $\text{YBa}_2\text{Cu}_3\text{O}_{6+y}$ as a function of oxygen activity (Ref. 12).

PURE OR DOPED?

If $\text{YBa}_2\text{Cu}_3\text{O}_6$ were an undoped compound and if the structure at this composition were the reference structure from which lattice defects are defined, the added oxygen would have to be placed in interstitial positions, i.e., in some of the sites that would have been occupied in a filled perovskite structure (assuming that cation vacancies are unfavorable defects by comparison). Our attempts to model the defect chemistry with oxygen interstitials have not been successful, and so we have taken the view that $\text{YBa}_2\text{Cu}_3\text{O}_6$ is the stoichiometric composition of a highly acceptor-doped compound and that the extra oxygen is filling oxygen vacancies that are present as compensating defects for the acceptor impurities.

MODEL

It will be assumed that YBCO is an acceptor-doped version of $\text{Y}_3\text{Cu}_3\text{O}_7$, a possibly hypothetical prototype. The rest of the defect model develops naturally from the single basic assumption that this is the composition of the stoichiometric, undoped prototype. Its structure should be the same as that of $\text{YBa}_2\text{Cu}_3\text{O}_7$, except for the replacement of two Ba^{2+} by Y^{3+} . The unoccupied oxygen sites, relative to the filled perovskite lattice, are not vacancies, but part of the structure. Therefore this is the structure from which lattice defects are defined. Ba^{2+} substituted for Y^{3+} serves as the acceptor, and the incorporation reaction can be expressed as



where it is understood that the two units of BaO replace the amount of Y_2O_3 shown in the parentheses above the reaction arrow. Charge neutrality is controlled by

$$[\text{Ba}'_{\text{Y}}] = 2[V_{\text{O}}^{\bullet\bullet}]. \quad (2)$$

The stoichiometric composition of the acceptor-doped composition is thus $\text{YBa}_2\text{Cu}_3\text{O}_6$, as defined above, and it contains one fillable oxygen vacancy per formula unit.

Both the prototype and the acceptor-doped version contain one monovalent and two divalent copper ions, and this is not changed by the addition of oxygen to the doped composition. As seen in Fig. 1, at high temperatures $\text{YBa}_2\text{Cu}_3\text{O}_6$ acts as a semiconductor with a modest band gap; the undoped prototype $\text{Y}_3\text{Cu}_3\text{O}_7$ would be expected to have a similar electronic structure.

The oxidation reaction can then proceed by the filling of some of the oxygen vacancies that are compensating the acceptor centers. Holes are introduced into the valence band as the incoming oxygen atoms pick up electrons to become oxygen ions:



This is the standard oxidation reaction proposed for a wide variety of acceptor-doped perovskite and perovskite-related compounds.^{13,14} Since the holes are assumed to be in the valence band, where they are all equivalent charge carriers, the formal oxidation states of the Cu ions do not change.

The mass-action expression for Eq. (3) can be rearranged to give

$$\frac{[\text{O}_{\text{O}}]p^2}{[V_{\text{O}}^{\bullet\bullet}]} = K_{\text{OX}} e^{-\Delta H_{\text{OX}}/kT} P(\text{O}_2)^{1/2}, \quad (4)$$

where $p = [h^{\bullet}]$, ΔH_{OX} is the standard enthalpy of the oxidation reaction per added oxygen, and $P(\text{O}_2)$ is the oxygen activity or partial pressure in atm. In spite of the large variation in oxygen content of YBCO, it will be assumed that the system behaves ideally and that Eq. (4) is a complete and accurate description of the system. (It will be shown in the Appendix that for small values of y it is necessary to take into account intrinsic ionization across the band gap.) This assumption is based on the philosophy that ideal behavior will be considered valid as long as it appears to work.

Because of the very high defect concentrations, it is necessary to take explicit account of the increase in $[\text{O}_{\text{O}}]$ and the decrease in $[V_{\text{O}}^{\bullet\bullet}]$ as oxygen is added to YBCO. For the representation of the system by $\text{YBa}_2\text{Cu}_3\text{O}_{6+y}$ and with concentrations in terms of the number of a given species per formula unit, the addition of y oxygen atoms to the stoichiometric composition will result in the addition of $2y$ holes to the valence band, according to Eq. (3). The six oxygens per unit cell in the stoichiometric composition are increased by y to give a total of $6+y$, and the one fillable oxygen vacancy per unit cell is decreased by y to $1-y$. Equation (4) can then be replaced by

$$\frac{(6+y)(4y^2)}{(1-y)} = K_{\text{OX}} e^{-\Delta H_{\text{OX}}/kT} P(\text{O}_2)^{1/2}. \quad (5)$$

The thermogravimetric data of Lindemer *et al.*¹⁰ are accurately fit for values of y above 0.25 by Eq. (5) with the following values for the adjustable parameters:

$$\frac{(6+y)y^2}{(1-y)} = 3.594 \times 10^{-4} e^{0.83/kT} P(\text{O}_2)^{1/2}. \quad (6)$$

Lines calculated from this expression are compared with

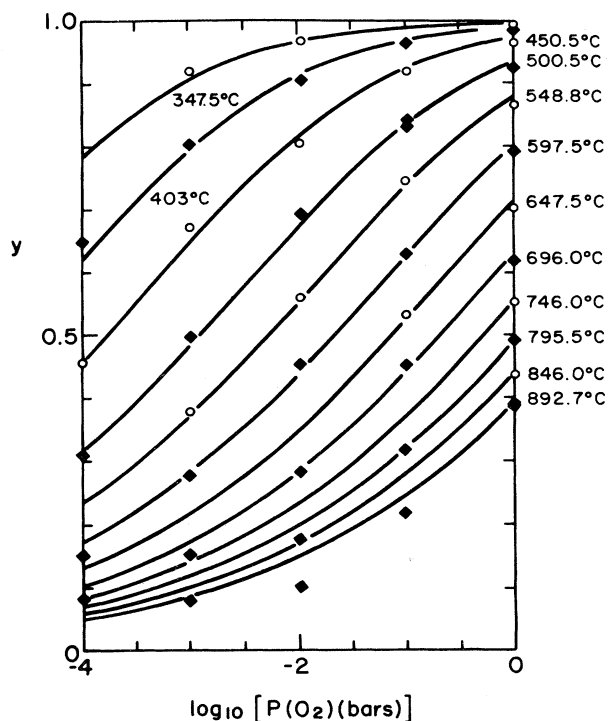


FIG. 2. Excess oxygen y in $\text{YBa}_2\text{Cu}_3\text{O}_{6+y}$ as a function of temperature and oxygen activity (Ref. 4). Data points from (10), lines calculated from Eq. (6).

the thermogravimetric data in Fig. 2, and values of the mass-action constant K'_{Ox} , calculated from the experimental data according to

$$K'_{\text{Ox}} = \frac{(6+y)y^2}{(1-y)P(\text{O}_2)^{1/2}}, \quad (7)$$

are plotted in Arrhenius form in Fig. 3. It is seen that the data are consistent with a single enthalpy of oxidation of -0.83 eV, which is close to values obtained from calorimetry,^{15,16} and the term $P(\text{O}_2)^{1/2}$ proves to be an accurate normalizing factor for the effect of oxygen activity.

The line in Fig. 3 is calculated from Eq. (6). In four cases on the Arrhenius plot, multiple data points overlap so strongly that they are represented by a single symbol, with the component data points for each indicated to the right of the plot. Five data points (out of 55 total) deviate significantly from the calculated line. As indicated, the three at high temperatures and low oxygen activities correspond to $(6+y) = 6.03, 6.08,$ and 6.10 ; i.e., the data are very close to the stoichiometric composition where intrinsic electronic ionization becomes important. It will be shown in the Appendix that inclusion of the latter effect is a rational correction for the discrepancies at low values of y . The other two points, at low temperatures and $P(\text{O}_2) = 1$ atm, correspond to $(6+y) = 6.992$ and 6.997 , so that $(1-y)$, the denominator of the mass-action expression, is the difference between two nearly equal numbers, and the accuracy of the calculation is greatly reduced. The fit of the calculated line to the experimen-

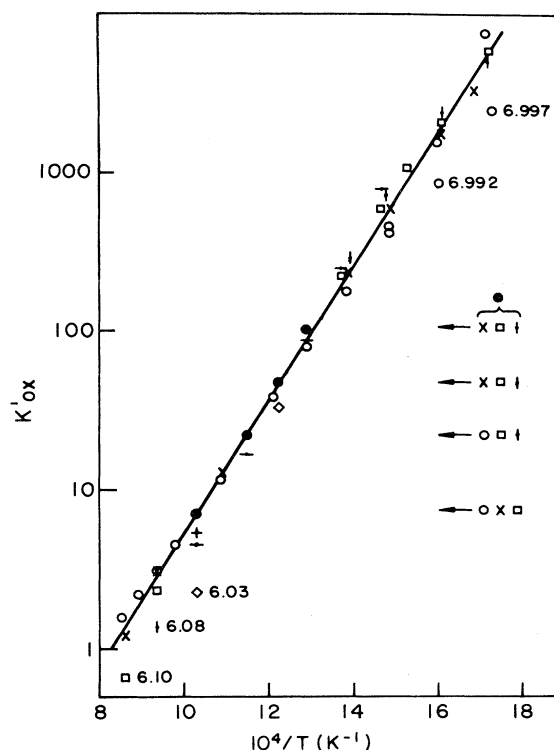


FIG. 3. Arrhenius plot of the mass-action constant K'_{Ox} for the oxidation reaction, Eq. (3), calculated from Eq. (7), using the data from Ref. 10. Oxygen activities in atm: \circ , 1; \times , 0.1; \square , 0.01; \circ , 10^{-3} ; \bullet , 10^{-4} . Multiple overlapping data points shown as \bullet , with component points shown on the right. Selected data points labeled with $(6+y)$.

tal data over the range $300\text{--}900^\circ\text{C}$ and $10^{-5}\text{--}1$ atm is superior to that of any other proposed defect model. The two adjustable parameters that define the slope and intercept of the Arrhenius plot are the minimum possible number. The ideal Arrhenius behavior demonstrated in Fig. 3 indicates that, for whatever reason, corrections for nonideality are not needed. This defect model is the simplest of all those proposed and follows well-established models for related systems.

DISCUSSION OF THE MODEL

If $\text{YBa}_2\text{Cu}_3\text{O}_6$ were a pure compound, as has been assumed to be in most defect models, it should be sensitive to aliovalent doping. Figure 4 shows the equilibrium conductivity of $\text{YBa}_{2-z}\text{La}_z\text{Cu}_3\text{O}_x$, with $z = 0, 0.1,$ and 0.2 ;¹¹ the latter two compositions correspond to a 5% and 10% replacement of Ba^{2+} by La^{3+} . It is seen that the dopant has essentially no effect on the equilibrium conductivity. This is consistent with the assumption that $\text{YBa}_2\text{Cu}_3\text{O}_6$ is already a highly acceptor-doped composition, so that the addition of La^{3+} is only reducing the net acceptor excess by 5% and 10%, respectively.

Figure 5 shows the concentrations of holes and oxygen vacancies as a function of $P(\text{O}_2)$, as calculated from Eq. (6). The usual experimental range is indicated by the ver-

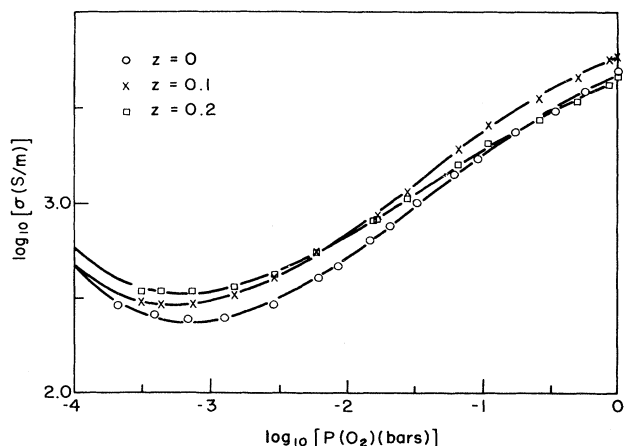


FIG. 4. Equilibrium conductivity of $\text{YBa}_{2-2}\text{La}_z\text{Cu}_3\text{O}_{6+y}$, as a function of oxygen activity at 800°C (Ref. 11).

tical lines. This clearly shows the replacement of oxygen vacancies by holes as the compensating defect as the oxygen content is increased. It also shows that the experimental data are taken in a transitional region where the limiting dependences on $P(\text{O}_2)$ are not fully developed. The flattening out of the equilibrium conductivity toward higher values of $P(\text{O}_2)$, as shown in Fig. 1, is seen to result from the near saturation of the available oxygen vacancies with added oxygen. The lines for the hole concentration in Fig. 5 look very much like the equilibrium conductivity lines in Fig. 1, except that no lines for electrons that would cause the conductivity minima at higher temperatures have been included. However, the model predicts that the maximum slope of $\log_{10} p$ vs $\log_{10} P(\text{O}_2)$ should be $\frac{1}{4}$, i.e., Eq. (4) with $[\text{O}_\text{O}] = 6$ and $[\text{V}'_\text{O}] = \frac{1}{2}[\text{Ba}'_\text{Y}]$, whereas the observed slopes for the conductivity at lower values of y are closer to $\frac{1}{2}$. This could be understood if the hole mobility were also proportional to $P(\text{O}_2)^{1/4}$, but there is no obvious reason for such a dependence. This remains an unexplained discrepancy between the defect model and the observed electrical conductivity. It has been stated that this model "is incapable of fitting the electrical properties."¹⁷ That is correct, as

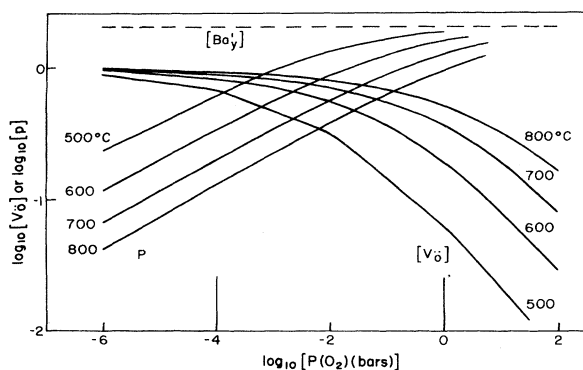


FIG. 5. Oxygen vacancy and hole concentrations in $\text{YBa}_2\text{Cu}_3\text{O}_{6+y}$, as a function of oxygen activity and temperature, calculated from Eq. (6).

described above, and it is also true of other proposed models, all of which require some *ad hoc* assumption to connect the compositional data with the electrical conductivity.

This defect model for YBCO is virtually identical to the one proposed earlier for acceptor-doped LaFeO_3 , $\text{La}_{1-x}\text{Sr}_x\text{FeO}_{3-x/2}$.¹⁸ The equilibrium conductivity of a sample with $x = 0.1$ is reproduced in Fig. 6. In this example, the stoichiometric composition is $\text{La}_{0.9}\text{Sr}_{0.1}\text{FeO}_{2.95}$, and it can be oxidized to $\text{La}_{0.9}\text{Sr}_{0.1}\text{Fe}[h]_{0.1}\text{O}_{3.00}$. Both systems show an exothermic oxidation reaction, an endothermic reduction reaction, and a conductivity minimum that is moving to higher $P(\text{O}_2)$ with increasing temperature. The exothermic (negative) enthalpies of oxidation are to be expected for acceptor-doped materials that have fillable oxygen vacancies and that have easily oxidized cations, i.e., Cu^+ and Fe^{3+} . Both compounds also show a leveling out of the hole concentration as the filling of the oxygen vacancy content approaches saturation. In the case of $\text{La}_{0.9}\text{Sr}_{0.1}\text{FeO}_{2.95}$, the conductivity has the expected proportionality to $P(\text{O}_2)^{1/4}$. Otherwise, the strikingly similar behavior for the two systems strongly suggests that they share a common defect model.

For $\text{La}_{1-x}\text{Sr}_x\text{FeO}_{3-x/2}$ with $x = 0.1$, the oxygen sublattice becomes completely filled by oxidation, and this is nearly so for a sample with $x = 0.25$. These two cases correspond to the filling of oxygen vacancies that amount to 1.7% and 4.3% of the total oxygen sites, respectively, and no need was found to correct for nonideal behavior. This compares with the filling of 16.7% of the oxygen sublattice in the case of the oxidation of $\text{YBa}_2\text{Cu}_3\text{O}_6$.

The model for $\text{YBa}_2\text{Cu}_3\text{O}_x$ requires that all of the holes created by the oxidation reaction be equivalent and distinct from any other species in the system. This would not be satisfied if Cu^+ were oxidized to Cu^{2+} or Cu^{3+} , or if Cu^{2+} were oxidized to Cu^{3+} , since both of these would result in changes in the concentrations of other species, in violation of the observed mass-action relationship. The behavior is resolved if all of the holes are placed in the valence band and the formal oxidation states of the

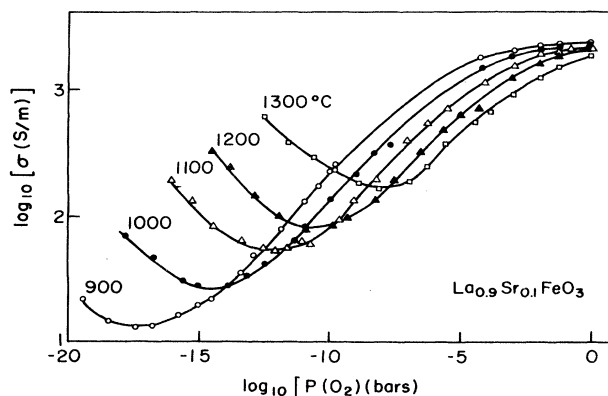
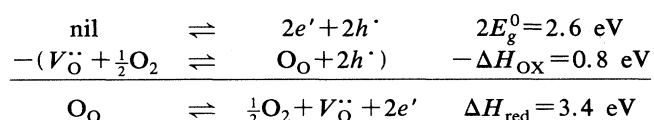


FIG. 6. Equilibrium conductivity of $\text{La}_{0.9}\text{Sr}_{0.1}\text{FeO}_3$ as a function of oxygen activity (from Ref. 18, reproduced with permission of the American Ceramic Society).

copper ions remain unchanged.

What are the criteria for the ideal behavior of a chemical system in equilibrium? It should be possible to substitute concentrations for activities; i.e., all activity coefficients should be unity, and the system should be described by a single standard free energy of reaction. The latter requires that an Arrhenius plot of the mass-action constant be linear. The proposed model for $\text{YBa}_2\text{Cu}_3\text{O}_x$ satisfies these criteria.

From the temperature dependence of the conductivity minima, an approximate value of 1.3 eV can be obtained for the band gap of YBCO (this is the band gap at 0 K, E_g^0 , or the enthalpy of the intrinsic ionization reaction). This can be combined with the enthalpy of the oxidation reaction to obtain a value for the enthalpy of the reduction reaction of about 3.4 eV,



This is a reasonable value for an oxide with an easily reducible cation such as Cu^{2+} .

CONCLUSION

Based on the single assumption that $\text{YBa}_2\text{Cu}_3\text{O}_6$ is the stoichiometric composition of an acceptor-doped version of $\text{Y}_3\text{Cu}_3\text{O}_7$, all major features of the defect chemistry of YBCO are accounted for quantitatively. Since the experimental results are fit by a single enthalpy of oxidation over the entire experimental range, the tetragonal-to-orthorhombic structural transition that has been reported to occur as a function of oxygen content must be a gradual, evolutionary change. This has been discussed in terms of local ordering of the variable oxygen content in this system.⁴ The model indicates that all of the holes created by oxidation are located in the valence band and that each formula unit contains one monovalent and two divalent copper ions, independent of the oxygen content. Although the defect concentrations are very high, the system fulfills all criteria for ideal thermodynamic behavior.

ACKNOWLEDGMENT

The authors are grateful for the support of the Division of Materials Research of the National Science Foundation.

APPENDIX: THE EFFECT OF INTRINSIC ELECTRONIC DISORDER

As described in the text and shown in Fig. 2, the agreement between Eq. (6) and the experimental data decreases with decreasing y for values below about 0.25. This is also seen in Fig. 3, where the values of the mass-action constants calculated from the experimental values for y fall below the line calculated from Eq. (6) when y is small, i.e., 0.03, 0.08, and 0.10. This discrepancy was attributed to the effect of intrinsic electronic ionization. Close to

TABLE I. Summary of results for the three discrepant data points in Fig. 3.

T (°C)	$P(\text{O}_2)$ (atm)	$6+y$	$2y$	K_i	$K_i^{1/2}$	p
700	10^{-5}	6.03	0.06	7.3×10^{-3}	0.085	0.12
800	10^{-3}	6.08	0.16	19×10^{-3}	0.14	0.24
900	10^{-2}	6.10	0.20	25×10^{-3}	0.16	0.29

stoichiometry, the oxidation reaction is not the only significant source of holes; additional holes result from intrinsic ionization across the band gap, and Eq. (6) does not take this additional source into account. It is of interest to see if this proposed explanation is reasonable.

The intrinsic ionization reaction is



for which the mass-action expression is

$$np = K_i, \quad (\text{A2})$$

where K_i has the temperature dependence of the band gap. Neglecting minority defects, the condition of charge neutrality is

$$2[V_{\text{O}}^{\cdot\cdot}] + p = n + [\text{Ba}'_{\text{Y}}]. \quad (\text{A3})$$

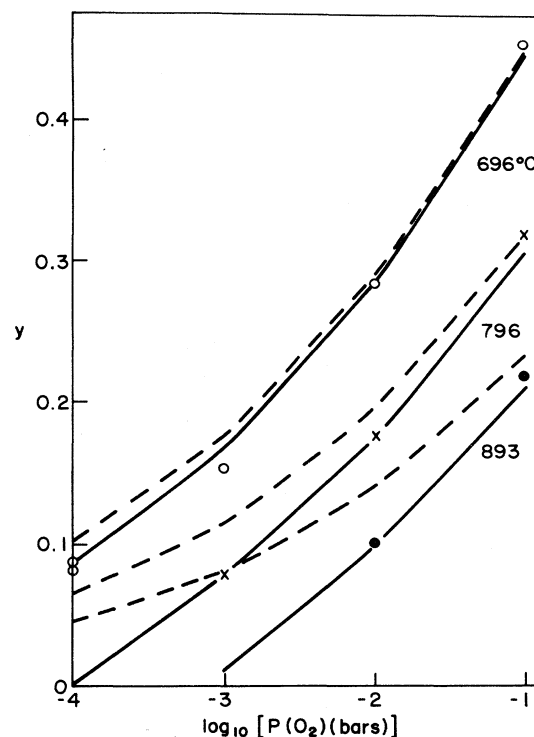


FIG. 7. Values of y at high temperatures and low oxygen activities corrected for intrinsic ionization. Dashed lines represent the uncorrected model, Eq. (6), while solid lines represent the corrected version, Eq. (A7). The symbols are from the thermogravimetric analysis (TGA) data of Ref. 10: \circ , 696°C; \times , 796°C; \bullet , 893°C.

Since $[V_{\text{O}}^{\bullet\bullet}] = 1 - y$ and $[\text{Ba}'_{\text{Y}}] = 2$, in the concentration units used in the test, this can be transformed into

$$p = n + 2y = K_i/p + 2y \quad (\text{A4})$$

This is consistent since at stoichiometry $y = 0$, so that $p = n$, while far from stoichiometry n is negligible and $p = 2y$. Solving this expression for p , substituting the result into Eq. (4), and solving for K_i gives

$$K_i = \left\{ \left[\frac{(1-y)K_p}{(6+y)} \right]^{1/2} P(\text{O}_2)^{1/4} - y \right\}^2 - y^2, \quad (\text{A5})$$

where K_p is the temperature-dependent mass-action constant,

$$K_p = 4K'_{\text{OX}} = K_{\text{OX}} e^{-\Delta H_{\text{OX}}/kT} \quad (\text{A6})$$

For the right-hand side of Eq. (A5), values for y and $P(\text{O}_2)$ are obtained from the experimental data for the three discrepant points, while K_p is calculated from Eq. (6). Values for p for these conditions can then be calculated from Eq. (A4). The results for the three points are summarized in Table I. Thus the true hole concentration p is larger than that attributed to the oxidation reaction, $2y$, by 50–100 %.

A more accurate mass-action expression can now be given by

$$\left[\frac{(6+y)}{(1-y)} \right] [y + (y^2 + K_i)^{1/2}]^2 = K_p P(\text{O}_2)^{1/2}, \quad (\text{A7})$$

and this can be used to fit the thermogravimetric data for small values of y . Calculated results obtained from Eqs. (6) and (A7) for 700, 800, and 900 °C are compared with

the experimental data in Fig. 7 (the actual data points were taken at the average temperatures of 696, 796, and 893 °C). The results corrected for intrinsic electronic ionization are in much better agreement.

The preceding derivation shows that inclusion of intrinsic electronic ionization is a reasonable correction for the deviations from experimental data observed for Eq. (6) for small values of y . Thus the combined mass-action treatment of the oxidation reaction and the intrinsic ionization reaction can give quantitative agreement with experiment over the entire range of the thermogravimetric data. The inclusion of intrinsic ionization implicitly includes the reduction reaction



since this can be obtained by subtracting the oxidation reaction, Eq. (3), from twice the intrinsic ionization reaction, Eq. (7). In fact, Eq. (A7) gives negative values for y for the most highly reducing conditions, consistent with a shift to the oxygen-deficient, n -type region seen in the equilibrium conductivity measurements in Fig. 1.

The derived mass-action constants for the intrinsic ionization reaction, K_i , were obtained from single data points and cannot be considered to be very accurate. Since y is small in the pertinent region 0.03–0.10, small experimental errors, e.g., 0.01, will have large effects on the derived values. However, the results suggest that if accurate values could be obtained for the mass-action constants for intrinsic electronic disorder as a function of temperature, the entire set of thermogravimetric data for $\text{YBa}_2\text{Cu}_3\text{O}_x$, with $6 < x < 7$, could be fit satisfactorily by the proposed model.

¹M.-Y. Su, S. E. Dorris, and T. O. Mason, *J. Solid State Chem.* **75**, 381 (1988).

²A. Mehta and D. M. Smyth, in *Non-Stoichiometric Compounds: Surfaces, Grain Boundaries, and Structural Defects*, edited by J. Nowotny and W. Weppner (Kluwer Academic, Dordrecht, 1989), pp. 509–520.

³E. K. Chang, A. Mehta, D. J. L. Hong, and D. M. Smyth, *Ferroelectrics* **102**, 309 (1990).

⁴D. J. L. Hong, A. Mehta, P. Peng, and D. M. Smyth, in *Superconductivity and Ceramic Superconductors*, Vol. 13 of *Ceramic Transactions*, edited by K. M. Nair and E. A. Giess (American Ceramic Society, Westerville, OH, 1990), pp. 129–147.

⁵J. Nowotny and M. Rekas, *J. Am. Ceram. Soc.* **73**, 1048 (1990).

⁶J. Nowotny and M. Rekas, *J. Am. Ceram. Soc.* **73**, 1054 (1990).

⁷D. J. L. Hong and D. M. Smyth, *J. Am. Ceram. Soc.* **74**, 1751 (1991).

⁸J. Nowotny and M. Rekas, *J. Am. Ceram. Soc.* **74**, 1753 (1991).

⁹J. Maier and H. L. Tuller, *Phys. Rev. B* **47**, 8105 (1993).

¹⁰T. B. Lindemer, J. F. Hunley, J. E. Gates, A. L. Sutton, Jr., J.

Brynstad, C. R. Hubbard, and P. K. Gallagher, *J. Am. Ceram. Soc.* **72**, 1775 (1989).

¹¹D. J. L. Hong, A. Mehta, D. M. Smyth, E. K. Chang, and M. J. Kirschner, *J. Mater. Res.* **5**, 1185 (1990).

¹²E. K. Chang, D. J. L. Hong, A. Mehta, and D. M. Smyth, *Mater. Lett.* **6**, 251 (1988).

¹³D. M. Smyth, *Prog. Solid State Chem.* **15**, 145 (1984).

¹⁴D. M. Smyth, in *Properties and Applications of Perovskite-Type Oxides*, edited by L. G. Tejuca and J. L. G. Fierro (Dekker, New York, 1993), pp. 47–72.

¹⁵L. R. Morss, D. C. Sonnenberger, and R. J. Thorn, *Inorg. Chem.* **27**, 2106 (1988).

¹⁶M. E. Parks, A. Navrotsky, M. Mocala, E. Takayama-Muromachi, A. Jacobson, and P. K. Davies, *J. Solid State Chem.* **79**, 53 (1989).

¹⁷T. O. Mason, in *Electronic Ceramic Materials*, edited by J. Nowotny (Trans Tech, Zurich, 1992), p. 528.

¹⁸J. Mizusaki, T. Sosamoto, W. R. Cannon, and H. K. Bowen, *J. Am. Ceram. Soc.* **66**, 247 (1983).